Ordered Macroporous Silica by Ice Templating

Hirotomo Nishihara,* Shin R. Mukai, Daisuke Yamashita, and Hajime Tamon

Department of Chemical Engineering, Kyoto University, Katsura, Nishikyo-ku, Kyoto 615-8510, Japan

Received August 2, 2004. Revised Manuscript Received September 24, 2004

Ordered macroporous silica, a silica gel microhoneycomb (SMH), has been prepared through a method which uses micrometer-sized ice crystals as a template. Template ice crystals, which have a continuous rod shape, a polygonal cross section, and ordered diameters, were grown inside precursor silica hydrogels under a condition where the pseudo-steady-state growth of them continues. Besides their ordered macroporosity, micro-/mesopores develop inside the honeycomb walls through the freeze-drying of SMHs soaked in *tert*-butyl alcohol. SMHs have straight and polygonal macroporous voids, which are created and retained through the formation and removal of the ice crystals. Micromorphology including macropore size and wall thickness, micro-/mesoporosity inside the honeycomb walls, and thermal stability of SMHs were investigated in detail through scanning electron microscopy observation, nitrogen adsorption−desorption measurements, and thermogravimetric analysis. It was found that the macropore size of the SMHs can be controlled by changing the immersion rate into a cold bath and the freezing temperature without changing the micro-/mesoporosity of their honeycomb walls. It was also found that the thickness of the honeycomb walls was affected by the SiO_2 concentration and the macropore size. On the other hand, the porosity of the honeycomb walls could be controlled to be microporous as well as mesoporous by hydrothermal treatment of as-prepared SMHs in basic aqueous solutions. Moreover, it was found that SMHs with developed mesopores showed a higher stability against heat treatment.

Introduction

Micro-/mesoporous materials are widely used as adsorbents, separation materials, or catalyst supports in various fields from large-scaled plants for water treatment to microdevices for advanced analysis.[1−3] In such applications, the performances of the micro-/mesoporous materials are strongly influenced not only by their micro-/mesoporosity but also by their morphology. There are various types of possible morphology that such materials can take, such as powder, granule, fiber, thin film, and honeycomb. The optimal morphology must be selected based on their application, taking into consideration of factors such as their filling density, sizes of diffusion paths within their structure, the pressure drop which is likely to occur during usage, etc. Recently, ordered macroporous materials with micro-/mesopores, which can be classified as a new morphology of micro-/mesoporous materials, have drawn great attention as they can be used as high-performance adsorbents, lightweight materials, and thermal, acoustic, and electrical insulators in the field of catalysis, photonics, chromatography, and large-molecule separation processes.[4−26] Ordered macroporous materials are generally prepared through templating methods. The use of colloidal crystal templates[4,5] of close-packed polymer or silica latex spheres can produce three-dimensionally ordered macroporous (3DOM) materials of metal oxides,[6−12] zeolites,[13,14] bioceramics,[15,16] metals,[17,18] polymers,[19,20] and other composites.[21−26] Such 3DOM materials have interconnected spherical macropores and are known to have unique optical properties and enhanced mass transfer

* To whom correspondence should be addressed. E-mail: nisihara@cheme.kyoto-u.ac.jp.

(1) Dabrowski, A. *Adv. Colloid. Interface Sci.* **2001**, *93*, 135−224.
(2) Davis, M. E. *Nature* **2002**, *417*, 813−821.
(3) Cooper, A. I. *Adv. Mater.* **2003**, *15*, 1049−1059.
(4) Velev, O. D.; Kaler, E. W. *Adv. Mater.* **2000**, *12*, 531−534.
(5) Kulinowski, K. M.; Jiang, P.; Vaswani, H.; Colvin, V. L. *Adv. Mater.* **2000**, *12*, 833−838.
(6) Velev, O. D.; Jede, T. A.; Lobo, R. F.; Lenhoff, A. M. *Nature* **1997**, *389*, 447−448.
(7) Velev, O. D.; Jede, T. A.; Lobo, R. F.; Lenhoff, A. M. *Chem. Mater.* **1998**, *10*, 3597−3602.
(8) Holland, B. T.; Blanford, C. F.; Stein, A. *Science* **1998**, *281*, 538−540.
(9) Wijnhoven, J. E. G. J.; Vos, W. L. *Science* **1998**, *281*, 802−804.
(10) Wang, D. Y.; Caruso, R. A.; Caruso, F. *Chem. Mater.* **2001**, *13*, 364−371.
(11) Wijnhoven, J. E. G. J.; Bechger, L.; Vos, W. L. *Chem. Mater.* **2001**, *13*, 4486−4499.
(12) Meng, Q. B.; Fu, C. H.; Einaga, Y.; Gu, Z. Z.; Fujishima, A.; Sato, O. *Chem. Mater.* **2002**, *14*, 83−88.
(13) Holland, B. T.; Abrams, L.; Stein, A. *J. Am. Chem. Soc.* **1999**, *121*, 4308−4309.
(14) Rhodes, K. H.; Davis, S. A.; Caruso, F.; Zhang, B. J.; Mann, S. *Chem. Mater.* **2000**, *12*, 2832−2834.
(15) Yan, H. W.; Zhang, K.; Blanford, C. F.; Francis, L. F.; Stein, A. *Chem. Mater.* **2001**, *13*, 1374−1382.
(16) Melde, B. J.; Stein, A. *Chem. Mater.* **2002**, *14*, 3326−3331.
(17) Wijnhoven, J. E. G. J.; Zevenhuizen, S. J. M.; Hendriks, M. A.; Vanmaekelbergh, D.; Kelly, J. J.; Vos, W. L. *Adv. Mater.* **2000**, *12*, 888−890.
(18) Sumida, T.; Wada, Y.; Kitamura, T.; Yanagida, S. *Langmuir* **2002**, *18*, 3886−3894.
(19) Jiang, P.; Hwang, K. S.; Mittleman, D. M.; Bertone, J. F.; Colvin, V. L. *J. Am. Chem. Soc.* **1999**, *121*, 11630−11637.
(20) Gates, B.; Yin, Y. D.; Xia, Y. N. *Chem. Mater.* **1999**, *11*, 2827−2836.
(21) Holland, B. T.; Blanford, C. F.; Do, T.; Stein, A. *Chem. Mater.* **1999**, *11*, 795−805.
(22) Yan, H. W.; Blanford, C. F.; Holland, B. T.; Smyrl, W. H.; Stein, A. *Chem. Mater.* **2000**, *12*, 1134−1141.
(23) Lebeau, B.; Fowler, C. E.; Mann, S.; Farcet, C.; Charleux, B.; Sanchez, C. *J. Mater. Chem.* **2000**, *10*, 2105−2108.
(24) Schroden R. C.; Blanford, C. F.; Melde, B. J.; Johnson, B. J. S.; Stein, A. *Chem. Mater.* **2001**, *13*, 1074−1081.
(25) Carreon, M. A.; Guliants, V. V. *Chem. Mater.* **2002**, *14*, 2670−2675.
(26) Al-Daous, M. A.; Stein, A. *Chem. Mater.* **2003**, *15*, 2638−2645.

10.1021/cm048725f CCC: $30.25
Published on Web 01/14/2005

abilities. Ordered macroporous materials with interconnected spherical macropores can also be prepared by using emulsion droplets[27−32] or polymer foam[33] as templates. Considering their applications in reaction or separation processes, it is desirable to synthesize them as large monoliths. Several efforts have been made to prepare large monolithic macroporous materials using these template methods.[14,31−33] Another approach to prepare such materials is a method using chemically induced phase separation and subsequent post-gelation.[34−39] In this method, the separated phase of polymer additive plays the role of a template. Macroporous silica monoliths derived from this method have been used as the stationary phase in HPLC and showed extremely higher performances compared with conventional columns packed with particles.[34,35] Their application to reaction processes is also beginning to be considered.[38,39]

Large monolithic macroporous materials can also be produced through cryochemical synthesis routes.[40−46] When hydrosols, hydrogels, or aqueous slurries of metal oxides or polymer are quickly frozen by immersing them into a cold bath, micrometer-sized ice spheres grow inside their matrixes as a result of thermally induced phase separation. These ice spheres play the role of a template, and three-dimensionally interconnected macroporous metal oxides or polymers can be prepared. In this "ice-templating" method, template ice spheres are formed in situ and can be easily removed simply through thawing and drying. Needing neither a special template material nor a special removal process of the template, this ice-templating method is inexpensive and environmentally friendly and can produce highly pure materials with interconnected spherical macropores. From these excellent advantages, this method can be used to produce highly pure micro-/mesoporous ceramics[41,42] and is popularly used to prepare scaffold materials in tissue engineering.[43−46] However, as the size of the template, ice spheres, is determined by freezing conditions, such as immersion rate into a cold bath and freezing temperature, and it is impossible to adjust such conditions to be completely uniform throughout the whole sample at the freezing stage, it is difficult to produce well-ordered macropores by using this ice-templating method.

We have discovered that it is possible to produce ordered macroporous materials through a modified ice-templating method, which uses the pseudo-steady-state growth of ice crystals.[47,48] When precursor hydrogels, which are freshly gelled and have an adequate amount of solid components within them, are unidirectionally frozen under a condition where pseudo-steady-state growth of ice crystals can continue, an array of polygonal ice rods with fairly uniform diameters grows in parallel with the freezing direction. After the removal of the template ice, large monolithic materials with ordered macropores can be obtained. The straight macropores have a polygonal cross section and are parallel to the freezing direction. We have also confirmed through ink-penetration tests that the macropores are not blocked. We named this novel micromorphology of the obtained materials as microhoneycomb because they have such structures as miniaturized honeycomb supports. Presently, we have succeeded in preparing monolithic silica gel microhoneycombs (SMHs),[47] organic gel microhoneycombs, and carbon gel microhoneycombs[48] by using this method. In this work, the controlling of the size of the macropores, wall thickness, and micro-/mesoporosity inside the honeycomb walls of SMHs are described in detail. The thermal stability of SMHs with different micro-/mesoporosity is also reported. Freeze-drying[49,50] has been used to dry the SMHs, and cryogels, which are highly micro-/mesoporous materials, like aerogels were obtained.[51] We intend to introduce this ice-templating method as a new method for the production of ordered macroporous materials with controllable micro-/mesoporosity.

Experimental Section

Preparation of SMHs. Commercial sodium silicate solutions (Wako, Japan) were diluted with distilled and deionized water, giving solutions of desired SiO_2 concentrations, C_s. Then the pH of the solutions was adjusted to 3 using an ion-exchange resin (Amberlite IR120B H AG, Organo, Japan). The obtained clear sols were poured into polypropylene tubes, which were 100 mm in length and 10 mm in diameter, and aged at 303 K. Next, the freshly gelled hydrogels were unidirectionally frozen by dipping the tubes at a constant rate of v_f into a cold bath maintained at a constant temperature of T_f. v_f and T_f were varied and their effects on the size of macropores of the resulting SMHs were investigated. It was confirmed that pseudo-steady-state ice growth initiated at least at about 50 mm from the bottom of the tubes and continued till the

(27) Imhof, A.; Pine, D. J. *Nature.* **1997**, *389*, 948−951.
(28) Manoharan, V. N.; Imhof, A.; Thorne, J. D.; Pine, D. J. *Adv. Mater.* **2001**, *13*, 447−450.
(29) Sen, T.; Tiddy, G. J. T.; Cascic, J. L.; Anderson, M. W. *Chem. Commun.* **2003**, *17*, 2182−2183.
(30) Shen, J. G. C. *J. Phys. Chem. B* **2004**, *108*, 41−51.
(31) Huerta, L.; Guillem, C.; Latorre, J.; Beltran, A.; Beltran, D.; Amoros, P. *Chem. Commun.* **2003**, *12*, 1448−1449.
(32) Maekawa, H.; Esquena, J.; Bishop, S.; Solans, C.; Chmelka, B. F. *Adv. Mater.* **2003**, *15*, 591−596.
(33) Lee, Y. J.; Lee, J. S.; Park, Y. S.; Yoon, K. B. *Adv. Mater.* **2001**, *13*, 1259−1263.
(34) Minakuchi, H.; Nakanishi, K.; Soga, N.; Ishizuka, N.; Tanaka, N. *Anal. Chem.* **1996**, *68*, 3498−3501.
(35) Tanaka, N.; Kobayashi, H.; Minakuchi, H.; Ishizuka, N. *Anal. Chem.* **2001**, *73*, 420A−429A.
(36) Liang, C. D.; Dai, S.; Guiochon, G. *Chem. Commun.* **2002**, *22*, 2680−2681.
(37) Smatt, J. H.; Schunk, S.; Linden, M. *Chem. Mater.* **2003**, *15*, 2354−2361.
(38) Nakamura, N.; Takahashi, R.; Sato, S.; Sodesawa, T.; Yoshida, S. *Phys. Chem. Chem. Phys.* **2000**, *2*, 4983−4990.
(39) Takahashi, R.; Sato, S.; Sodesawa, T.; Yabuki, M. *J. Catal.* **2001**, *200*, 197−202.
(40) Sofie, S. W.; Dogan, F. *J. Am. Ceram. Soc.* **2001**, *84*, 1459−1464.
(41) Koch, D.; Andresen, L.; Schmedders, T.; Grathwohl, G. *J. Sol-Gel Sci. Technol.* **2001**, *26*, 149−152.
(42) Zhang, B. J.; Davis, S. A.; Mann, S. *Chem. Mater.* **2002**, *14*, 1369−1375.
(43) Zhang, R. Y.; Ma, P. X. *J. Biomed. Mater. Res.* **1999**, *44*, 446−455.
(44) Madihally, S. V.; Matthew, H. W. T. *Biomaterials* **1999**, *20*, 1133−1142.
(45) Kang, H. W.; Tabata, Y.; Ikada, Y. *Biomaterials* **1999**, *20*, 1339−1344.
(46) Chen, G. P.; Ushida, T.; Tateishi, T. *Adv. Mater.* **2000**, *12*, 455−457.
(47) Mukai, S. R.; Nishihara, H.; Tamon, H. *Chem. Commun.* **2004**, *7*, 874−875.
(48) Nishihara, H.; Mukai, S. R.; Tamon, H. *Carbon* **2004**, *42*, 899−901.
(49) Tamon, H.; Ishizaka, H.; Yamamoto, T.; Suzuki, T. *Carbon* **1999**, *37*, 2049−2055.
(50) Mukai, S. R.; Nishihara, H.; Tamon, H. *Microporous Mesoporous Mater.* **2003**, *63*, 43−51.
(51) Pierre, A. C.; Pajonk, G. M. *Chem. Rev.* **2002**, *102*, 4243−4265.

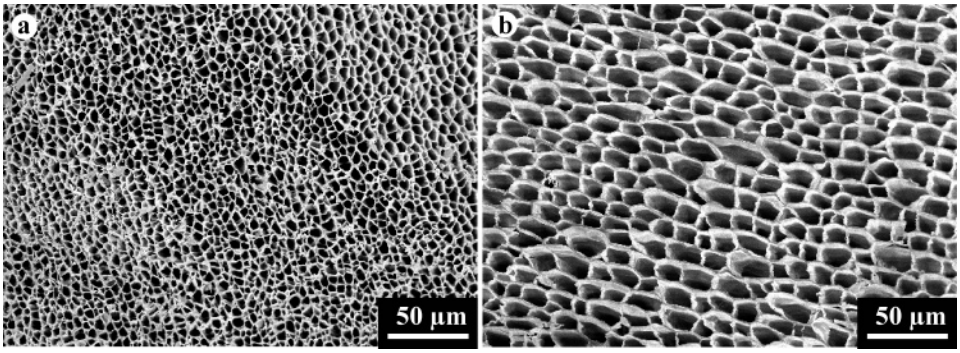

Figure 1. SEM images of the cross sections of silica gel microhoneycombs having different macropore sizes, which were prepared through different immersion rates of (a) 20 cm/h and (b) 6 cm/h at 77 K.

Table 1. Preparation Conditions and the Physical Properties of SMHs

sample	C_s[a] (mol/L)	T_f[b] (K)	v_f[c] (cm/h)	average macropore size (μm)	average wall thickness (μm)	S_{BET}[d] (m^2/g)	V_{mes}[e] (cm^3/g)	d_{peak}[f] (nm)
SMH-3	1.9	77	50	3.6	0.28	nm[g]	nm	nm
SMH-4	1.9	77	20	4.7	0.32	869	0.06	<2
SMH-5	1.9	77	6	17	0.74	818	0.05	<2
SMH-6	1.9	213	6	42	2.13	nm	nm	nm
SMH-7	1.6	77	20	4.9	0.22	nm	nm	nm
SMH-8	1.0	77	6	19	0.62	898	0.11	<2

[a] SiO_2 concentration of the parent sol. [b] Freezing temperature. [c] Immersion rate into a cold bath. [d] BET specific surface area. [e] Mesopore volume calculated by applying Dollimore-Heal method to the adsorption isotherm. [f] Peak diameter of mesopore size distribution. [g] Not measured.

tubes were completely frozen, in all cases. Next, the samples were transferred to a cold bath maintained at 243 K and were kept in it for 2 h in order to strengthen their structure in a state where ice crystals act as templates. After this low-temperature aging, the parts obtained through pseudo-steady-state ice growth were cut out and thawed at 323 K. Hydrothermal treatments were applied to some of the thawed SMHs and their effects on the micro-/mesoporosity of the resulting SMHs were investigated. Thawed SMHs were immersed in aqueous NH_3 solutions (two concentrations of 0.1 and 1.0 mol/L were used) and were kept at various temperatures (T_{ht}) for 5 days. The hydrothermally treated samples or simply thawed samples were then immersed into 10-times their volumes of *tert*-butyl alcohol and were kept there for over 1 day in order to exchange the water included in their structure with *tert*-butyl alcohol. This washing operation was repeated three times. Next, the wet samples were freeze-dried at 263 K, and finally dry samples maintaining their wet-state nano-/microstructures were obtained. To investigate the effect of heat treatment on the micro-/mesoporosity of the SMHs, they were heat-treated at 878 and 1178 K for 2 h in an air flow, and the changes in their micro-/mesoporosity were compared.

Characterization. The micromorphology of the SMHs was observed by a scanning electron microscope (JEOL Japan Inc.; JSM-6340FS), and the average macropore size and average wall thickness of each SMH were determined from the obtained micrographs. Micro-/mesoporosity inside the honeycomb walls of the SMHs was evaluated by analyzing their N_2 adsorption−desorption isotherms measured at 77 K using an adsorption apparatus (BEL Japan Inc.; BELSORP28). BET surface areas, S_{BET}, were calculated through the Brunauer−Emmett−Teller (BET) method, and mesopore size distributions and mesopore volumes, V_{mes}, were calculated through the Dollimore-Heal method applied to the adsorption isotherms. Note that the range of mesopore size used in the calculation of V_{mes} is 2−50 nm in diameter, as defined by IUPAC. Thermal stability of the SMHs were characterized using a thermogravimetric analyzer (Shimadzu Co.; TGA-50). The samples were heated to 1273 K in a nitrogen atmosphere at a heating rate of 10 K/min.

Results and Discussion

Macropore Sizes of SMHs. Figure 1 shows SEM images of the cross section of SMHs, which were prepared using different immersion rates (SMH-4 and SMH-5 in Table 1). Since the cross section of the macropores of SMHs has a well-ordered honeycomb structure, our proposed ice-templating method might be associated with the Widawski's method, which uses water droplets as templates to produce thin polymer membranes with well-ordered spherical or honeycomb macropores.[52−54] Both their method and ours use H_2O as templates and do not need template additives or special processes to remove them. However, formation mechanisms of templates in their method and ours are completely different. Their template, spherical water droplets, generates from the water-saturated vapor on cooled surfaces of water-immiscible solvents.[55−57] On the other hand, our template, ice crystals with polygonal rod shape, generates inside the hydrogels by phase separation. Therefore, the shapes of resulting macropores are also different. Long, straight macropores can be formed through the ice-templating method (Figure 2), while spherical macropores are formed when water droplets are used as the template. Moreover, SMHs can be molded not only into thin films but also into large monoliths, which are thought to be suitable for applications such as catalysts, catalyst supports, adsorbents, and stationary phase of HPLC.

(52) Widawski, G.; Rawiso, M.; François, B. *Nature* **1994**, *369*, 387−389.
(53) Pitois, O.; François, B. *Eur. Phys. J. B* **1999**, *8*, 225−231.
(54) Pitois, O.; François, B. *Colloid Polym. Sci.* **1999**, *277*, 574−578.
(55) Karthaus, O.; Maruyama, N.; Cieren, X.; Shimomura, M.; Hasegawa, H.; Hashimoto, T. *Langmuir* **2000**, *16*, 6071−6076.
(56) de Boer, B.; Stalmach, U.; Nijland, H.; Hadziioannou, G. *Adv. Mater.* **2000**, *12*, 1581−1583.
(57) Srinivasarao, M.; Collings, D.; Philips, A.; Patel, A. *Science* **2001**, *292*, 79−83.

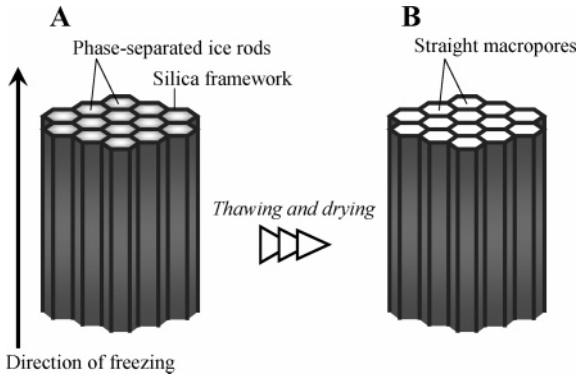

Figure 2. Model which illustrates the formation of macropores by ice templating. (A) The microstructure formed by the phase separation during unidirectional freezing of silica hydrogels. An array of straight ice rods with polygonal cross sections is formed. Silica framework is formed at the interspace of the ice rods. (B) After removal of the ice rods by thawing and drying, macropores are formed as a replica of the ice rods.

Figure 1 shows that a faster immersion rate produces smaller macropores. Since the macropores of SMHs are a replica of the ice rods, the difference in macropore sizes, which can be noticed in Figure 1, proves that the sizes of the ice rods were affected by immersion rates. Therefore, the macropore sizes of the SMHs can be controlled indirectly by changing the sizes of the ice rods. Mahler et al. pointed out that the freezing of hydrogels and the solidification of eutectic alloys are similar phenomena.[58] It is reported that when a melt alloy is unidirectionally solidified and a cellular structure appears, the intercellular spacing can be expressed as a function of $(GR)^{-1}$, where G is the temperature gradient in the liquid−solid interface and R is the solidification velocity.[59] Therefore, in the freezing of hydrogels, the macropore sizes are also thought to be affected by these factors. To confirm this, we prepared SMHs under various v_f and T_f conditions and measured their macropore sizes as shown in Table 1. From the data of SMH-3 to 6, the effects of these two parameters on the size of macropores can be clearly realized. On the other hand, the size of the macropores was found to be hardly affected by the SiO_2 concentration of the parent sol, C_s (see the data of SMH-4 and 7, and the data of SMH-5 and 8 in Table 1). Assuming G is proportional to $T_r - T_f$ (T_r is room temperature), we plotted the size of macropores of the SMHs against $\{v_f(T_r - T_f)\}^{-1}$ as shown in Figure 3. It can be seen that the size of macropores can be expressed as a function of $\{v_f(T_r - T_f)\}^{-1}$.

The size of macropores in ordered macroporous materials is very important, as it could extremely affect mass transfer abilities and the pressure drop which is likely to occur during their usage. Therefore, it is desirable to tune the size of macropores according to their applications. In the production of 3DOM materials, the size of macropores can be controlled by changing the size of template latex spheres.[6] We showed that the size of macropores of SMHs can be easily and precisely controlled in a wide range of 3−40 μm by simply adjusting v_f and T_f. Therefore, ordered macroporous materials prepared through the ice-templating method are expected to be used in various applications.

(58) Mahler, W.; Bechtold, M. F. *Nature* **1980**, *285*, 27−28.
(59) Flemings, M. C. *Solidification processing*; McGraw-Hill: New York, 1974.

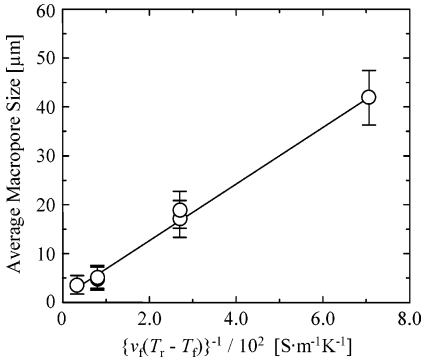

Figure 3. Relationship between the average macropore sizes of silica gel microhoneycombs and $\{v_f(T_r - T_f)\}^{-1}$; v_f is immersion rate into a cold bath, T_r is room temperature, and T_f is freezing temperature.

Wall Thickness of SMHs. It can be seen that v_f and C_s do not affect the micro-/mesoporosity of the honeycomb walls from the data of SMH-4, 5, and 8 in Table 1. Indeed we have confirmed that all of the N_2 isotherms of these samples are practically identical. The reason for such consequences can be explained by the concentration effect, which is induced by freeze-gelation.[50] In the preparation of porous silica gels through freeze-gelation, it has also been confirmed that the freezing temperature does not affect the micro-/mesoporosity of the resulting material. Therefore, the ratio of the total volume of honeycomb walls against the total volume of ice crystals should increase with the increase in C_s; i.e., the wall thickness of the SMHs is expected to increase with the increase in C_s. On the other hand, it can be easily noticed that the wall thickness of SMHs will increase with the increase in macropore size, i.e., the increase in $\{v_f(T_r - T_f)\}^{-1}$, at the same volume ratio of the honeycomb walls. Figure 4 shows enlarged SEM images of SMHs with different wall thicknesses (SMH-6 and SMH-7 in Table 1). It can be seen that the wall thickness of (a) is about 10 times that of (b). The wall thicknesses of the samples are summarized in Table 1. It can be noticed that the wall thickness can be increased by increasing the macropore size, d_{mac}, and C_s. Interestingly, by plotting the wall thicknesses of SMHs against the product of C_s and d_{mac}, a fairly straight line could be obtained as shown in Figure 5. It can be seen that the wall thickness can be expressed as a function of C_s d_{mac}, which can be regarded as a useful parameter for the controlling of the wall thickness of SMHs.

In conventional methods which use templates for the preparation of 3DOM materials, the wall thickness is often limited by the void spaces of the preformed template architecture. Therefore, to control the wall thickness, it is necessary to form core−shell building blocks before colloidal crystallization.[14] We just showed that it is possible to control the wall thickness in this ice-templating method by changing $\{v_f(T_r - T_f)\}^{-1}$ or C_s. Controlling the wall thickness by changing C_s is thought to be effective since the wall thickness can be changed without changing the macropore size of the SMHs.

It was found that the macropore size of the SMHs can be controlled by v_f and T_f, and the wall thickness of the SMHs can be changed by v_f, T_f, and C_s. As v_f, T_f, and C_s do not affect the micro-/mesoporosity of the resulting SMH, it can be concluded that the micromorphology of SMHs can be

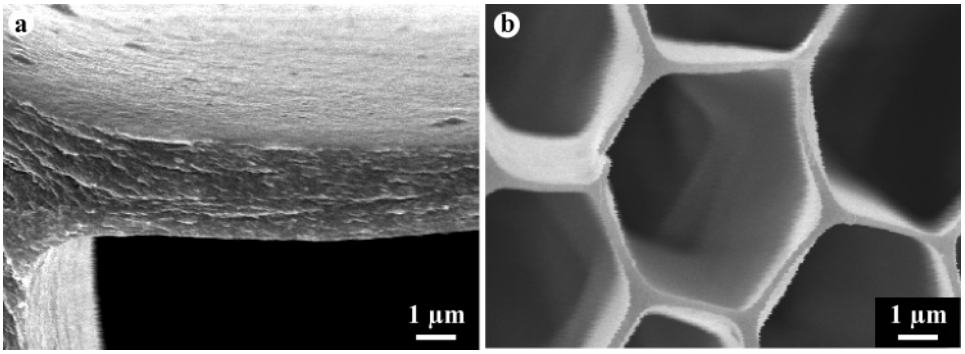

Figure 4. SEM images of the cross sections of silica gel microhoneycombs with different wall thicknesses. The samples were prepared under different immersion rates (v_f), freezing temperatures (T_f), and SiO_2 concentrations (C_s); (a) $v_f = 6$ cm/h, $T_f = 213$ K, and $C_s = 1.9$ mol/L; (b) $v_f = 20$ cm/h, $T_f = 77$ K, and $C_s = 1.6$ mol/L.

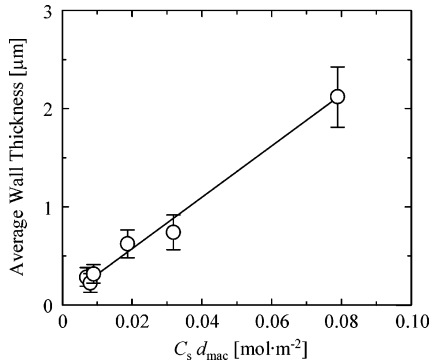

Figure 5. Relationship between the average wall thickness of silica gel microhoneycombs and $C_s\, d_{mac}$; C_s is SiO_2 concentration of the parent sol, d_{mac} is average macropore sizes of silica gel microhoneycombs.

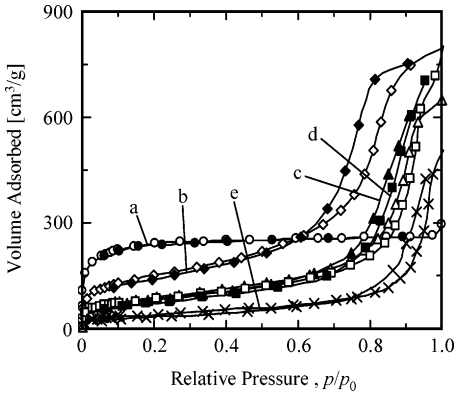

Figure 6. Nitrogen adsorption−desorption isotherms of silica gel microhoneycombs hydrothermally treated in NH_3 *aq*. of different concentrations of C_N at different temperatures of T_{ht}. (a) No treatment, (b) $C_N = 0.1$ mol/L and $T_{ht} = 298$ K, (c) $C_N = 0.1$ mol/L and $T_{ht} = 323$ K, (d) $C_N = 1.0$ mol/L and $T_{ht} = 323$ K, and (e) $C_N = 1.0$ mol/L and $T_{ht} = 363$ K.

controlled independently from their micro-/mesoporosity by adjusting these three parameters.

Micro-/Mesoporosity inside the Honeycomb Walls. SMHs prepared through the proposed ice-templating method have extremely low apparent density (ca. 0.12 g/cm^3), which are similar to those of silica aerogels. On the other hand, the density of the walls of SMHs is about 1.2 g/cm^3, which is close to those of conventional silica gels. Moreover, we have confirmed through X-ray diffraction measurements that the walls of SMHs have an amorphous structure like conventional silica gels. Therefore, it is expected that the conventional methods for the controlling of micro-/mesoporosity of silica gels can be applied to SMHs. We have actually showed that it is possible to change the micro-/mesoporosity of the walls of SMHs by changing the pH of their parent sols.[47] However, the pH affects the gelation time of silica sols, and the firmness of the resulting silica hydrogels. At a pH around 5, the gelation time becomes too short and the hydrogels tend to become too firm to transform into a microhoneycomb structure. Therefore, there is a pH region where a microhoneycomb structure cannot be obtained. This means that it is difficult to precisely control the micro-/mesoporosity of SMHs only by changing the pH of their parent sols. In this work, we applied another method, hydrothermal treatment, to precisely control the micro-/mesoporosity of SMHs in a wide range. When silica gels with micro-/mesopores are immersed into a basic solution, "Ostwald ripening" proceeds; i.e., smaller nanoparticles which compose the silica gel matrixes dissolve and reprecipitate on the surface of larger nanoparticles.[60] As a result, the average size of the pores increases. With application of this method, the micro-/mesoporosity of SMHs is expected to be controlled independently from their macroporosity since this process can be easily applied after the ordered macropores are already formed.

SMHs were formed through unidirectional freezing and after thawing they were immersed into NH_3 solutions of designated concentrations of C_N and were cured for 5 days at designated temperatures of T_{ht}. Nitrogen isotherms and mesopore size distributions of SMHs, which were hydrothermally treated, are compared with those of SMHs which were not treated in Figure 6 and Figure 7, respectively. Moreover, the effects of C_N and T_{ht} on the micro-/mesoporosity of the resulting SMHs are summarized in Table 2. Though SMH-a, which was not hydrothermally treated, shows a type I isotherm, other SMHs show type IV isotherms, which indicates that these samples have developed mesopores (Figure 6). By applying hydrothermal treatment to SMHs, the sizes of the micro-/mesopore inside the honeycomb walls could be varied in a wide range of $2<$ to 45 nm (Table 2). With comparison of the shapes of the isotherms in the low relative pressure range (Figure 6), and the BET surface areas, S_{BET}, (Table 2) it can be concluded that microporosity decreases with the increase in T_{ht}. On the other hand, the sizes of the mesopores increase, and mesopore

(60) Brinker, C. J.; Scherer, G. W. *Sol−gel science*; Academic Press: San Diego, 1990.

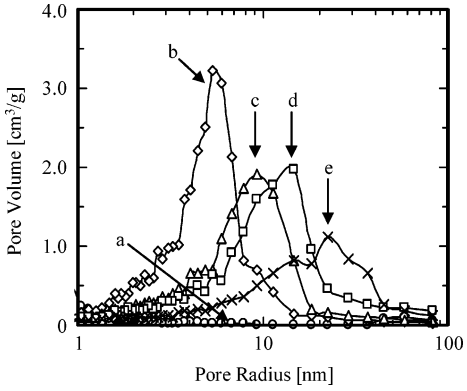

Figure 7. Mesopore size distributions of silica gel microhoneycombs hydrothermally treated in NH_3 *aq*. of different concentrations of C_N at different temperatures of T_{ht}. (a) No treatment, (b) $C_N = 0.1$ mol/L and $T_{ht} = 298$ K, (c) $C_N = 0.1$ mol/L and $T_{ht} = 323$ K, (d) $C_N = 1.0$ mol/L and $T_{ht} = 323$ K, and (e) $C_N = 1.0$ mol/L and $T_{ht} = 363$ K.

Table 2. Effects of Hydrothermal Treatment and Heat Treatment on the Micro-/Mesoporosity of Silica Gel Microhoneycombs

sample	C_N[a] (mol/L)	T_{ht}[b] (K)	calcination temperature (K)	S_{BET}[c] (m^2/g)	V_{mes}[d] (cm^3/g)	d_{peak}[e] (nm)
SMH-a				877	0.06	<2
SMH-a600			873	nd[f]	nd	nd
SMH-b	0.1	298		533	1.19	10.8
SMH-c	0.1	323		308	0.93	18.6
SMH-d	1.0	323		291	1.00	26.6
SMH-e	1.0	363		143	0.51	44.9
SMH-e600	1.0	363	873	145	0.53	44.9
SMH-e900	1.0	363	1173	108	0.49	44.9

[a] NH_3 concentration of solution used for hydrothermal treatment. [b] Hydrothermal treatment temperature. [c] BET specific surface area. [d] Mesopore volume calculated by applying Dollimore-Heal method to the adsorption isotherm. [e] Peak diameter of mesopore size distribution. [f] Not detected.

size distribution broadens with the increase in T_{ht} (Figure 7). The effects of C_N on the micro-/mesoporosity of the resulting SMHs were much different from that of T_{ht}. Only the mesopore size changed with the increase in C_N. Therefore, it can be said that it is possible to increase mesopore size, without changing the mesopore volume and the sharpness of the distribution, by increasing C_N, the results being consistent with previous reports.[61]

Heat Stability of SMHs. Besides the unique straight shape of controllable macropores, whose sizes can be easily controlled, SMHs have controllable micro-/mesopores inside their honeycomb walls. Therefore, SMHs are expected to be used in various reaction and separation processes as a porous material whose pressure drop hardly occurs during usage. Considering their uses in such applications, the heat stability of them is very important. For example, catalytic reaction processes are usually conducted at high temperatures. Moreover, to use SMHs for applications such as the stationary phase for HPLC, SMHs might need to be calcined before their actual usage to stabilize their surface properties or to remove impurities. From Table 2, it can be seen that the heat stability of SMHs is affected by their micro-/mesoporosity. The microporosity of the honeycomb walls of SMH-a, which was not hydrothermally treated and has

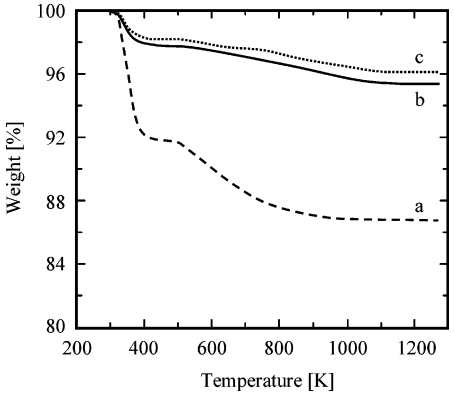

Figure 8. TGA curves of silica gel microhoneycombs hydrothermally treated in NH_3 *aq*. of different concentrations of C_N at different temperatures of T_{ht}. (a) No treatment, (b) $C_N = 1.0$ mol/L and $T_{ht} = 323$ K, and (c) $C_N = 1.0$ mol/L and $T_{ht} = 363$ K.'

almost no mesopores, significantly dropped by heat treatment. This sample showed no micro-/mesoporosity after heat treatment at 873 K. On the other hand, the micro-/mesoporosity of the honeycomb walls of SMH-e, which was hydrothermally treated thoroughly and has large mesopores, did not decrease at all by heat treatment at 873 K, and still showed porosity even after heat treatment to temperatures up to 1173 K. Therefore, we examined in detail the heat stability of the SMHs with different micro-/mesoporosity by TGA. Figure 8 shows TGA curves of as-synthesized samples (SMH-a, d, and e in Table 2). Weight loss is observed mainly in two temperature regions. The first significant weight loss, which is observed in each sample from room temperature to around 423 K, corresponds to the desorption of physisorbed water. The second significant weight loss, which is observed above 493 K, corresponds to dehydration induced by condensation of silanol groups. It was confirmed that the degree of dehydration in SMH-a is much larger than those of SMH-d and e. Moreover, it can be seen that there is a correlation between the amount of dehydration and micro-/mesopore size. It was found that the heat stability of SMHs increases with the increase in the sizes of micro-/mesopores in their honeycomb walls.

Conclusions

In this work, we showed that the ice-templating method we developed could be a new processing technology for the preparation of ordered macroporous materials with micro-/mesoporosity. We showed that it is possible to precisely control the macroporosity, wall thickness, and micro-/mesoporosity of SMHs obtained through this method by extremely simple procedures. When compared with conventional methods used for the preparation of ordered macroporous materials, the ice-templating method has many advantages: (a) it gives materials with straight and ordered macropores, so significant pressure drop during its usage can be avoided. (b) It gives crack-free materials with monolithic shape. (c) It does not require the addition of special templates which usually leads to high production costs in conventional methods. And (d) it does not require severe processes to remove templates, such as calcination and chemical etching, using a strong base. Therefore, it can be said that this ice-

(61) Nakanishi, K.; Takahashi, R.; Naganake, T.; Kitayama, K.; Koheiya, N.; Shikata, H.; Soga, N. *J. Sol-Gel Sci. Technol.* **2000**, *17*, 191−210.

templating method is a highly practical method which allows the production of ordered macroporous materials with high purity and advanced function.

Acknowledgment. This research was partially supported by the Japan Society for the Promotion of Science, Grant-in-Aid for Scientific Research (C), No. 15760569 (2003) and Grant-in-Aid for Scientific Research (B), No. 16360383 (2004), and the Micro Chemical Plant Technology Union (MCPT) for the Project of Micro-Chemical Technology for Production, Analysis, and Measurement Systems provided by the New Energy and Industrial Technology Development Organization (NEDO) of Japan.

CM048725F